Suspended tungsten trioxide (WO_3) gate AlGaN/GaN heterostructure deep ultraviolet detectors with integrated micro-heater

Sun, Jianwen; Zhan, Teng; Liu, Zewen; Wang, Junxi; Yi, Xiaoyan ; Sarro, Pasqualina M.; Zhang, Guoqi

DOI
10.1364/OE.27.036405

Publication date
2019

Document Version
Final published version

Published in
Optics Express

Research Article | Vol. 27, No. 25 / 9 December 2019 / Optics Express 36405

Optics EXPRESS

Suspended tungsten trioxide (WO_3) gate AlGaN/GaN heterostructure deep ultraviolet detectors with integrated micro-heater

JIANWEN SUN,[1,8] TENG ZHAN,[2,3,8] ZEWEN LIU,[4,7] JUNXI WANG,[2,3] XIAOYAN YI,[2,3] PASQUALINA M. SARRO,[1,5] AND GUOQI ZHANG[1,3,6]

[1] *Department of Microelectronics, Delft University of Technology, 2628 CD Delft, Netherlands*
[2] *Research and Development Center for Solid State Lighting, Institute of Semiconductors, Chinese Academy of Sciences, Qinghua East Road 35A, 100083, Beijing, China*
[3] *State Key Laboratory of Solid State Lighting, Beijing, 100083, China*
[4] *Institutue of Microelectronic, Tsinghua University 100084, Beijing, China*
[5] *p.m.sarro@tudelft.nl*
[6] *G.Q.Zhang@tudelft.nl*
[7] *liuzw@tsinghua.edu.cn*
[8] *These authors contributed equally to this paper.*

Abstract: A suspended WO_3-gate AlGaN/GaN heterostructure photodetector integrated with a micro-heater is micro-fabricated and characterized for ultraviolet photo detection. The transient optical characteristics of the photodetector at different temperatures are studied. The 2DEG-based photodetector shows a recovery (170 s) time under 240 nm illumination at 150 °C. The measured spectral response of WO_3-gate AlGaN/GaN heterostructure shows a high response in deep ultraviolet range. Responsivity at 240 nm wavelength is 4600 A/W at 0.5 V bias. These characteristics support the feasibility of a high accuracy deep UV detector based on the suspended AlGaN/GaN heterostructure integrated with a micro-heater.

1. Introduction

The ultraviolet (UV) spectral region is commonly classified by electromagnetic radiation with a wavelength range from 100 nm to 400 nm. It can be divided into UVA (315-400 nm), UVB (280-315 nm) and UVC (100-280 nm). Solar blind (wavelength shorter than 290 nm) photodetectors have widespread applications including flame sensing [1], missile and rocket plume monitoring [2], communication systems [3], space detection [4], UV environmental monitoring and so forth. Recently, some valuable researches have been made in AlGaN-based UV detectors [5,6]. Several types detector configurations, including PIN diodes [7,8], Schottky -type diodes [9] and metal semiconductor metal (MSM) [10–12] based photodetectors have been fabricated and demonstrated for UV detection. GaN based UV detectors can operate under harsh environment due to their wide bandgap material properties compared to silicon-based UV photodetectors. In comparison with other UV detectors, AlGaN/GaN heterostructure type detectors have an advantage of high gain, which is introduced by the high mobility two-dimensional electron gas (2DEG) channel at the surface of GaN layer.

An AlGaN/GaN HEMT based UV detector with a maximum responsivity of ~3000 A/W was first reported by Khan [13]. In recent years, responsivity values of $\sim 10^7$ A/W under 365 nm illumination have been demonstrated [14,15]. It is found that the drain current and the 2DEG channel conductivity of AlGaN/GaN HEMTs increase under UV light illumination. The mechanism of AlGaN/GaN HEMT UV detection has been reported before [16,17]. Several reports have considered 365 nm light illumination change the charge status of surface states and alter the conductivity of the 2DEG channel [16]. Others consider that accumulation of

#378929 https://doi.org/10.1364/OE.27.036405
Journal © 2019 Received 2 Oct 2019; revised 8 Nov 2019; accepted 11 Nov 2019; published 27 Nov 2019

negative charges in the surface states, acting as virtual gate, are released under 325 nm UV light illumination, resulting to the increase of drain current [17]. So far very few results of deep UV detector with AlGaN/GaN HEMT device have been reported.

Persistent photoconductivity (PPC) effect associated with a 2DEG in an AlGaN/GaN heterostructure devices has been observed, which makes the device sensitive to light. However, the recovery time (decay time) of GaN-based optical photodetector is measured about hours to days after removing the UV illumination [18], which is a difficult problem for application which require reliable and consistent operation [19]. The decay time can be suppressed by raised temperatures which increase the carrier capture rate [18,20,21]. External power units can be used to achieve the required temperature. However, it is may not be feasible for some applications. Therefore, integrated a heating unit is an attractive alternative to mitigate the PPC effect.

Tungsten trioxide (WO_3) is a typical n-type semiconductor material and has excellent optoelectronic properties for UV detection. The mechanism of detection is introduced and explained by surface oxygen adsorption-desorption process [22]. The WO_3-based photodetectors [23] showed a fast and stable response, with high sensitivity to UV photodetection.

In this research, we demonstrate the successful realization of a suspended WO_3-gate AlGaN/GaN heterostructure deep ultraviolet photodetectors integrated with micro-fabricated heater, reported for the first time. The deep ultraviolet photodetector, including the AlGaN/GaN device and micro-heater unit, was suspended from the silicon substrate for thermal isolation. The temperature of the membrane is modulated by the micro-heater unit based on Joule heating. The transient characteristics of the photodetector at different temperatures are studied. The photodetector shows a rapid response and recovery time under 240 nm illumination. The measured spectral response of AlGaN/GaN heterostructure shows the high response in the deep UV range. These results support the AlGaN/GaN heterostructure platform to develop reliable deep ultraviolet photodetectors.

2. Experimental

Figure 1 presents a schematic drawing of the device cross-section. The AlGaN/GaN sensor is placed together with the microheater surrounding the active area on a suspended membrane. The contact pads are on the thick silicon frame. The AlGaN/GaN heterostructure was grown on a 2-inch silicon <111 > 1 mm-thick wafers using Metal-organic Chemical Vapor Deposition (MOCVD). It consisted of a 2 μm-thick undoped GaN buffer layer, followed by a 1 nm-thick AlN interlayer, an undoped 25 nm-thick $Al_{0.26}Ga_{0.74}N$ barrier layer, and a 3 nm-thick GaN epitaxial

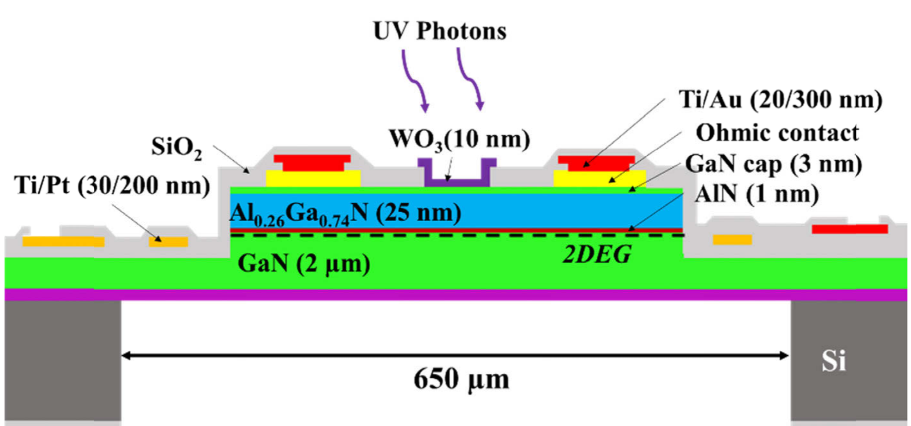

Fig. 1. Schematic drawing of the cross-section of the AlGaN/GaN UV photodetector.

cap layer. The electron mobility of 2DEG was ~1500 $cm^2/V \cdot s$, with a sheet electron density of ~$1 \times 10^{13} cm^{-2}$. The silicon substrate (400 μm) is backside etched by deep reactive ion etching (DRIE) to form a circular membrane (650μm in diameter).

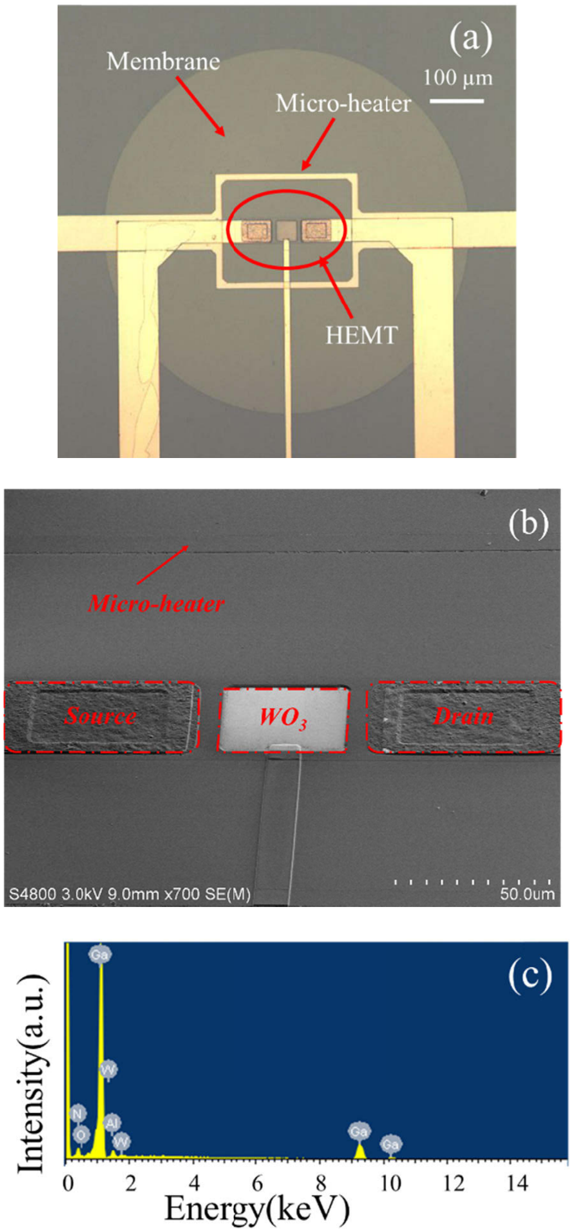

Fig. 2. The fabricated AlGaN/GaN UV photodetector (a) Top optical micrograph; (b) SEM image of device structure; (c) EDS spectrum of gate surface of device.

The fabrication process flow started with a mesa etching using a chlorine/boron chloride (Cl_2/BCl_3) inductively coupled plasma (ICP) to define the sensor geometry. Then, Ti/Al/Ti/Au (20/110/40/50 nm) metal contacts were e-beam evaporated and patterned by lift-off technology. After patterning, the contacts were subjected to a rapid thermal anneal at 870°C for 45 s under

Optics EXPRESS

N_2 ambient. 200-nm Silicon dioxide (SiO_2) was then deposited by plasma-enhanced chemical vapor deposition (PECVD). A Ti/Pt (30/200 nm) metal layer was evaporated and patterned by lift-off to form the microheater, followed by a 200-nm PECVD SiO_2 layer for isolation from the interconnect layer. After opening window of SiO_2 layer, the metal interconnect was formed using an evaporated Ti/Au (20/300 nm) layer stack. The topside of the wafer was covered by PECVD SiO_2 layer and the backside was polished down to 400 µm. A 5 µm-thick SiO_2 layer on the backside of wafer as hard mask during the DRIE process to etch the silicon substrate, was deposited and patterned by ICP etching. The topside SiO_2 layer was etched in BOE solution to open the contact pads and gate windows.

The WO_3 (10 nm) layer was deposited on the gate area of 40 µm x 40 µm by physical vapor deposition (PVD). The Silicon substrate is etched away below the active area in the final step. The microheater has a rectangular geometry around a central area of 230 µm x 290 µm, as showed in Fig. 2(a). Figure 2(b) shows the SEM images of the AlGaN/GaN device.The energy dispersive spectrum (EDS) of the device gate area surface is reported in Fig. 2(c). The corresponding peaks of Ga, W, N, Al, O elements are observed. Clearly, the deposition of WO_3 on the gate surface by magnetron sputtering is confirmed. More details about the device could been found in our early publication [24].

The spectral response of the AlGaN/GaN photodetectors was measured in a testing system (DSR200, Zolix Instrument Co., Ltd., China) under the monochromatic light with wavelength from 200 to 400 nm at a drain-source voltage of 0.5 V controlled by Keithley 2400 in air ambient at room temperature. The illuminating source is adopted by a 150 W Xenon lamp. The light source power measurements were calibrated using a Si detector. The schematic of spectral response measurement setup is shown in Fig. 3.

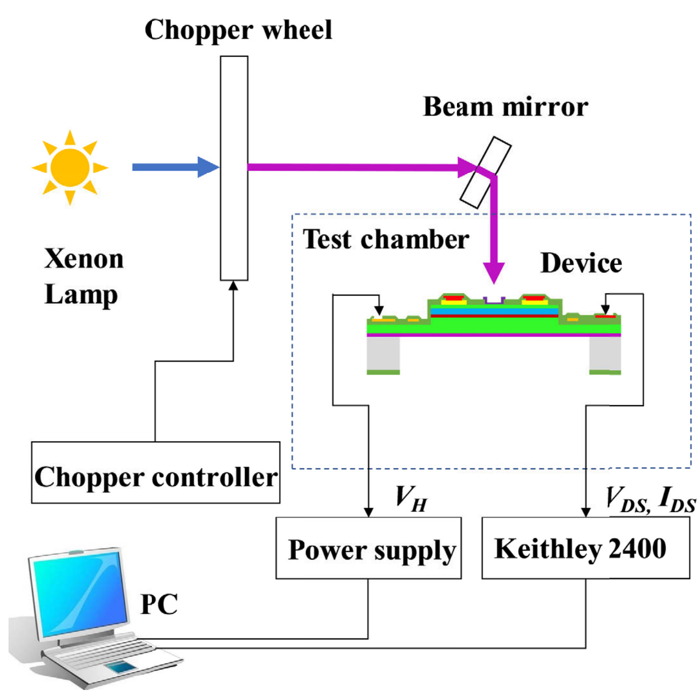

Fig. 3. A schematic of the spectral response measurement setup.

Optics EXPRESS

3. Results and discussion

The micro-heater filament increases the temperature by Joule heating when the current pass the filament. To extract the membrane temperature a calibration of the membrane temperatures at various heating voltages is necessary. The surface temperature can be measured by infrared radiation (IR) thermal camera or extracted by the resistance change of the micro-heater at ambient temperature with the 4-wire testing method [25]. Figure 4 shows the measured maximum temperatures of the AlGaN/GaN heterostructure photodetector at different applied micro-heater voltages. An infrared camera (Bruker) was used to record the temperature profile of the chip heated at V_H=4 V as shown in the inset of Fig. 4. A uniform profile across the membrane was observed.

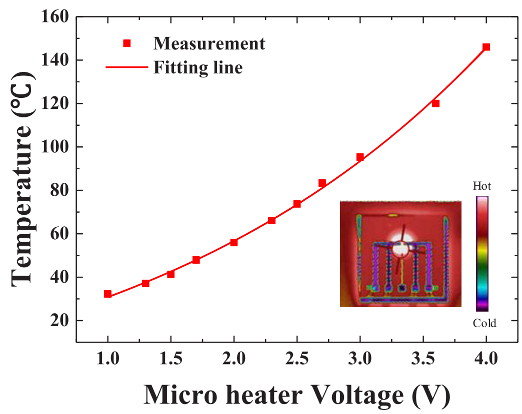

Fig. 4. Measurement of the heating temperature at different applied voltages. The inset shows the temperature profile (infrared camera image) of the heated (4 V) AlGaN/GaN photodetector.

WO_3 is an n-type semiconductor [23,26] and Fig. 5 shows the corresponding UV sensing mechanisms on the energy band diagram. When there is no bias applied between the source and drain of the detector in the dark, the oxygen molecules from the ambient air absorbed on the nanolayer WO_3, combine with electrons and create a depletion sub-layer near the surface [O_2(gas)+ $e^- \rightarrow O_2^-$(adsorb)], where O_2^- is the adsorbed oxygen ion on the WO_3 surface. So that there is depletion layer in the nanolayer WO_3 surface, as shown in Fig. 5. Under the deep UV light illumination conditions, more electron-hole pairs are photogenerated inside the WO_3. Then the generated holes move towards the WO_3 surface to recombine with the electrons trapped in O_2^- ions [h^++ O_2^-(adsorb)$\rightarrow$ O_2(gas)], [26] which help the adsorbed oxygen ions desorb from the WO_3 surface and decrease the width of the depletion layer. Therefore, the negative potential on the WO_3 nanolayer is reduced and 2DEG concentration in the channel layer of heterostructure is enhanced. Hence, the drain-source current is increased under deep UV illumination, as shown in Fig. 5 and Fig. 6.

The transient photocurrent response and normalized transient drain current responses of the suspended AlGaN/GaN heterostructure detectors under 240 nm UVC light illumination, at various applied micro-heater voltages, are shown in Fig. 6(a) and 6(b).

For the transient responses, the photo-to-dark-current ratio (PDCR) is defined as follows:

$$\mathrm{PDCR} = \frac{I_p - I_d}{I_d} \tag{1}$$

where I_p is the photo current under illumination and I_d is the dark current. The PDCR calculated values were approximately 0.034, 0.04 and 0.07 when micro-heater voltage was applied by 0 V, 2

Optics EXPRESS

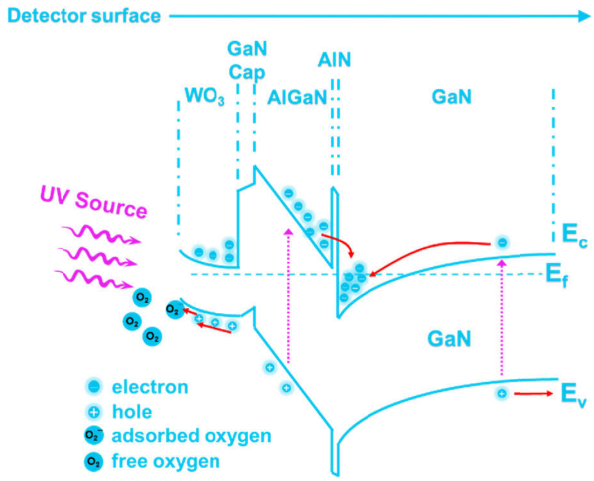

Fig. 5. Schematic illustration of the band diagram to describe the AlGaN/GaN heterostructure photodetector with WO_3 layer, E_f and dashed line denote the Femi level.

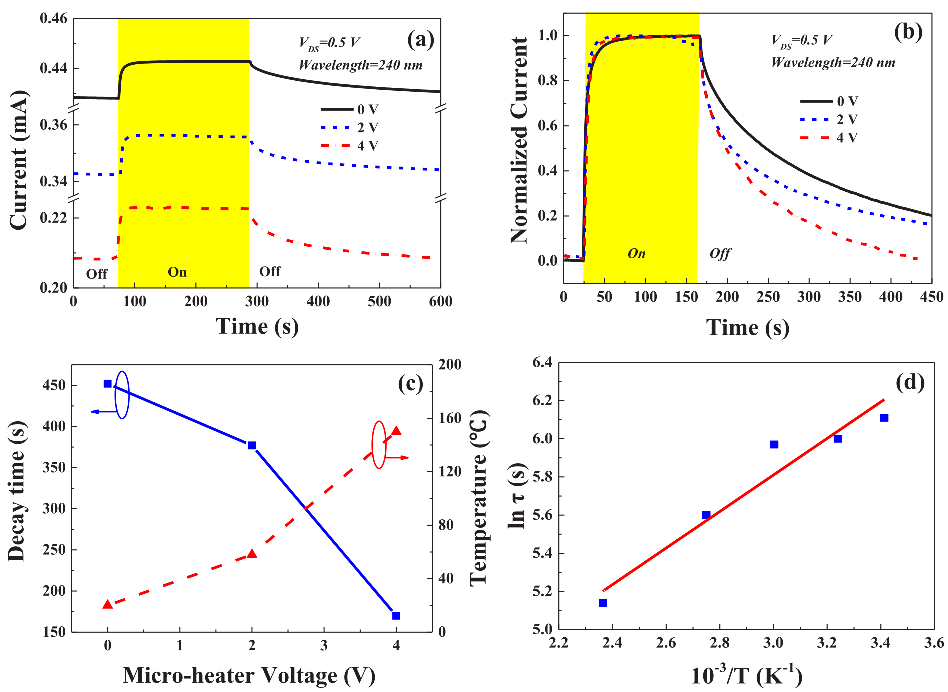

Fig. 6. Transient photocurrent response (a) and Normalized transient photocurrent response (b) of suspended AlGaN/GaN photodetector at various applied micro-heater voltages ($V_{micro-heater}$=0 V, 2 V, 4 V). Normalized photocurrent values: 0% is dark and 100% is maximum photocurrent under 240 nm illumination. The measured decay time and temperature of membrane at various micro-heater voltages are shown in (c). (d) Arrhenius plot of the PPC decay time constant at different temperatures.

V and 4 V, respectively. The relatively low PDCR values of detectors measured in this study are resulted from the low intensity of the Xenon lamp at wavelength of 240 nm (~1.26 mW/cm^2) [21].

Optics EXPRESS

Another reason is that larger dark current due to the high source-drain current of AlGaN/GaN 2DEG HEMT structure compared to p-i-n and Schottky structure. The photodetector shows a rapid response (8.4 s) under illumination, but the photocurrent decay depends on the applied micro-heater voltages. The decay time of photodetector is defined as the time required for the photo current changes from 90% to 10% of its saturated response value. The Fig. 6(c) shows the decay time decreases with increasing applied micro-heater voltages. The decay time is about 450 s at V_H=0 V (temperature was about 20 °C), and is suppressed to about 170 s when the photodetector is heated to approximately 150 °C at V_H=4 V (~280 mW). The decay time could be further reduced by increasing the micro-heater voltage (temperature) or a short time heating process (thermal relaxion) [27]. With the increasing temperature, electrons get more thermal energy, and the electron capture rate increases, reducing the decay times of device [21]. The power and voltage of heating unit can be further optimized by the membrane size and layout.

Earlier research has proposed the following model to describe the temperature dependency of the decay time constant (τ), which can be described by Eq. (2)

$$\tau = \tau_0 e^{(\Delta E/\mathrm{K}T)} \tag{2}$$

Where τ_o is the high temperature limit of the time constant, K is the Boltzmann constant, ΔE is the capture barrier and T is the temperature. The electron capture energy ΔE shown in Fig. 6(d) of approximately 160 meV is calculated. The carrier capture barrier prevents the decay of photoexcited electrons. The carrier capture barrier has been proposed to originate from the non-overlapping vibronic states of unfilled and filled defects. From electrons in conduction band require additional energy to get into the vibronic states of filled defects in order to be captured. As electrons gain more thermal energy with rising temperature, the electron capture rate increases, and thus the decay times of the photodetectors are reduced.

The spectral response of WO_3/AlGaN/GaN device shows the high response in the solar-blind range with wavelength of 210 ~280 nm, corresponding to the absorption area of the WO_3 nanolayer [23]. The peak responsivity was 4600 A/W at 0.5 V bias under 240 nm UVC illumination, which exceeds 100% quantum efficiency due to the high gain of HEMT 2EDG structure. As shown in Fig. 7, a transition is observed near the GaN cut-off wavelength at ~360 nm. The excellent performance of our devices is a clear indication of the potential applicability this configuration has for deep ultraviolet photodetectors.

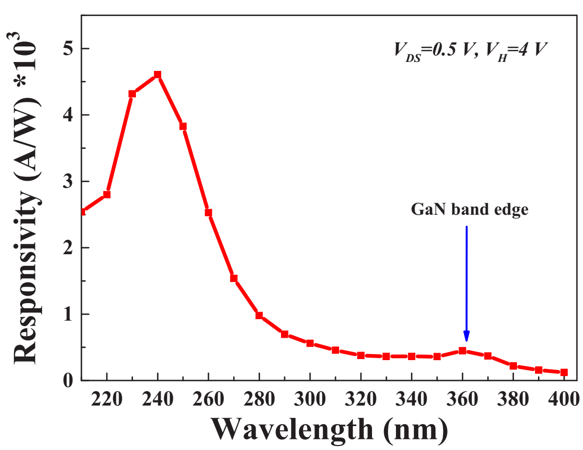

Fig. 7. The measured spectral response of AlGaN/GaN HEMT photodetector at V_{DS}=0.5 V, V_H=4 V.

4. Conclusions

In summary, suspended WO_3 gate AlGaN/GaN heterostructure deep ultraviolet photodetector integrated with a micro-heater were fabricated and characterized. The transient optical characteristics of the photodetector at different temperatures are studied. The photodetector shows a rapid response (8.4 s) and recovery (170 s) time under 240 nm illumination at 150°C. The spectral response of AlGaN/GaN device shows the high response in the deep ultraviolet range with a cut-off wavelength (280 nm). Responsivity at the wavelength of 240 nm was 4600 A/W at 0.5 V bias. These characteristics of the here presented suspended AlGaN/GaN devices integrated with a micro-heater, form an encouraging first step towards the development of a high accuracy and fast response 2DEG-based deep ultraviolet detector.

Funding

National Key Research and Development Program of China (2017YFB0403100, 2017YFB0403105, 2017YFB0403103).

Acknowledgments

Jianwen Sun and Teng Zhan contributed equally to this paper. The authors would like to thank the staff of the Institute of Semiconductor, Chinese Academy of Sciences for their assistance in device fabrication, and Suxia Zhang and Gang Sun from Zolix Instrument Co., LTD for optical testing.

Disclosures

The authors declare no conflicts of interest.

References

1. R. A. Miller, H. So, T. A. Heuser, and D. G. Senesky, "High-temperature Ultraviolet Photodetectors: A Review," arXiv preprint arXiv:1809.07396 (2018).
2. A. Blanc, L. Deimling, and N. Eisenreich, "UV- and IR-Signatures of Rocket Plumes," Propellants, Explos., Pyrotech. **27**(3), 185–189 (2002).
3. Z. Y. Xu and B. M. Sadler, "Ultraviolet communications: Potential and state-of-the-art," IEEE Commun. Mag. **46**(5), 67–73 (2008).
4. J. L. Robichaud, "SiC optics for EUV, UV, and visible space missions," in Future EUV/UV and Visible Space Astrophysics Missions and Instrumentation (International Society for Optics and Photonics 2003), pp. 39–50.
5. E. Munoz, E. Monroy, J. L. Pau, F. Calle, F. Omnes, and P. Gibart, "III nitrides and UV detection," J. Phys.: Condens. Matter **13**(32), 7115–7137 (2001).
6. P. E. Malinowski, J. John, J. Y. Duboz, G. Hellings, A. Lorenz, J. G. R. Madrid, C. Sturdevant, K. Cheng, M. Leys, J. Derluyn, J. Das, M. Germain, K. Minoglou, P. De Moor, E. Frayssinet, F. Semond, J. F. Hochedez, B. Giordanengo, and R. Mertens, "Backside-Illuminated GaN-on-Si Schottky Photodiodes for UV Radiation Detection," IEEE Electron Device Lett. **30**(12), 1308–1310 (2009).
7. B. Butun, T. Tut, E. Ulker, T. Yelboga, and E. Ozbay, "High-performance visible-blind GaN-based p-i-n photodetectors," Appl. Phys. Lett. **92**(3), 033507 (2008).
8. T. Tut, T. Yelboga, E. Ulker, and E. Ozbay, "Solar-blind AlGaN-based p-i-n photodetectors with high breakdown voltage and detectivity," Appl. Phys. Lett. **92**(10), 103502 (2008).
9. K. H. Lee, P. C. Chang, S. J. Chang, Y. C. Wang, C. L. Yu, and S. L. Wu, "AlGaN/GaN Schottky Barrier UV Photodetectors With a GaN Sandwich Layer," IEEE Sens. J. **9**(7), 814–819 (2009).
10. C. K. Wang, S. J. Chang, Y. K. Su, Y. Z. Chiou, S. C. Chen, C. S. Chang, T. K. Lin, H. L. Liu, and J. J. Tang, "GaN MSM UV photodetectors with titanium tungsten transparent electrodes," IEEE Trans. Electron Devices **53**(1), 38–42 (2006).
11. R. W. Chuang, S. P. Chang, S. J. Chang, Y. Z. Chiou, C. Y. Lu, T. K. Lin, Y. C. Lin, C. F. Kuo, and H. M. Chang, "Gallium nitride metal-semiconductor-metal photodetectors prepared on silicon substrates," J. Appl. Phys. **102**(7), 073110 (2007).
12. C. K. Wang, Y. Z. Chiou, S. J. Chang, W. C. Lai, S. P. Chang, C. H. Yen, and C. C. Hung, "GaN MSM UV Photodetector With Sputtered AlN Nucleation Layer," IEEE Sens. J. **15**(9), 4743–4748 (2015).
13. M. A. Khan, M. S. Shur, Q. Chen, J. N. Kuznia, and C. J. Sun, "Gated Photodetector Based on Gan/Algan Heterostructure Field-Effect Transistor," Electron. Lett. **31**(5), 398–400 (1995).

14. S. J. Chang, T. M. Kuan, C. H. Ko, Y. K. Su, J. B. Webb, J. A. Bardwell, Y. Liu, H. Tang, W. J. Lin, Y. T. Cherng, and W. H. Lan, "Nitride-based 2DEG photodetectors with a large AC responsivity," Solid-State Electron. **47**(11), 2023–2026 (2003).
15. B. Poti, M. T. Todaro, M. C. Frassanito, A. Pomarico, A. Passaseo, M. Lomascolo, R. Cingolani, and M. De Vittorio, "High responsivity GaN-based UV detectors," Electron. Lett. **39**(24), 1747–1749 (2003).
16. Y. C. Chang, "Effects of illumination on the excess carrier dynamics and variations of the surface states in an AlGaN/GaN heterostructure," J. Appl. Phys. **107**(3), 033706 (2010).
17. R. Vetury, N. Q. Zhang, S. Keller, and U. K. Mishra, "The impact of surface states on the DC and RF characteristics of AlGaN/GaN HFETs," IEEE Trans. Electron Devices **48**(3), 560–566 (2001).
18. J. Z. Li, J. Y. Lin, H. X. Jiang, M. A. Khan, and Q. Chen, "Persistent photoconductivity in a two-dimensional electron gas system formed by an AlGaN/GaN heterostructure," J. Appl. Phys. **82**(3), 1227–1230 (1997).
19. E. Monroy, F. Calle, J. L. Pau, E. Munoz, F. Omnes, B. Beaumont, and P. Gibart, "AlGaN-based UV photodetectors," J. Cryst. Growth **230**(3-4), 537–543 (2001).
20. C. H. Qiu and J. I. Pankove, "Deep levels and persistent photoconductivity in GaN thin films," Appl. Phys. Lett. **70**(15), 1983–1985 (1997).
21. M. M. Hou, H. Y. So, A. J. Suria, A. S. Yalamarthy, and D. G. Senesky, "Suppression of Persistent Photoconductivity in AlGaN/GaN Ultraviolet Photodetectors Using In Situ Heating," IEEE Electron Device Lett. **38**(1), 56–59 (2017).
22. D. L. Shao, M. P. Yu, J. Lian, and S. Sawyer, "Optoelectronic properties of three dimensional WO3 nanoshale and its application for UV sensing," Opt. Mater. **36**(5), 1002–1005 (2014).
23. Z. Hai, M. K. Akbari, C. Y. Xue, H. Y. Xu, L. Hyde, and S. Zhuiykov, "Wafer-scaled monolayer WO3 windows ultra-sensitive, extremely-fast and stable UV-A photodetection," Appl. Surf. Sci. **405**, 169–177 (2017).
24. J. Sun, R. Sokolovskij, E. Iervolino, F. Santagata, Z. Liu, P. M. Sarro, and G. Zhang, "Characterization of an Acetone Detector Based on a Suspended WO3-Gate AlGaN/GaN HEMT Integrated With Microheater," IEEE Trans. Electron Devices **66**(10), 4373–4379 (2019).
25. C. Silvestri, P. Picciafoco, B. Morana, F. Santagata, G. Q. Zhang, and P. M. Sarro, "Electro-thermal simulation and characterization of vertically aligned CNTs directly grown on a suspended microhoplate for thermal management applications," Ieee Sensor (2014).
26. K. Huang, Q. Zhang, F. Yang, and D. He, "Ultraviolet photoconductance of a single hexagonal WO 3 nanowire," Nano Res. **3**(4), 281–287 (2010).
27. H. Zhou, L. Cong, J. Ma, B. Li, M. Chen, H. Xu, and Y. Liu, "High gain broadband photoconductor based on amorphous Ga 2 O 3 and suppression of persistent photoconductivity," J. Mater. Chem. C **7**(42), 13149–13155 (2019).